AN EXPERIMENTAL INVESTIGATION OF THE TURBULENT TRANSFER OF HEAT IN THE INITIAL AND STABILIZED SEGMENTS OF A CYLINDRICAL TUBE UNDER CONDITIONS OF SUBSTANTIAL NONISOTHERMICITY

A. I. Leont'ev, B. P. Mironov, and A. V. Fafurin

UDC 536.244

We present experimental data on the transfer of heat in the initial and main segments of a cylindrical tube over a wide range of variation for the enthalpy factor $\psi_h = 0.08-0.8$ and the Reynolds number ($Re_{d_0} = 6.9 \cdot 10^3 - 2.4 \cdot 10^5$). The experimental data are generalized with a single relationship.

Of great interest in engineering practice are the problems associated with the determination of the heat transfer and friction under conditions in which a wall to be cooled is streamlined by a high-temperature gas. Despite the rather large number of investigations, this problem has not yet been adequately studied [1-7]. Thus, for example, the results from a number of investigations yield uncoordinated and even contradictory data, and no studies have been carried out for the initial segment of a tube under these conditions. No systematic research has been carried out on the effect of the enthalpy factor on heat transfer and friction over a broad range of variation in that factor under the identical conditions achievable through a single test installation. As a result of this it is extremely difficult to arrive at a reliable conclusion regarding the change in heat transfer and friction under conditions of nonisothermicity.

It is the purpose of this paper to obtain experimental data on the transfer of heat in the initial and stabilized segments of a cylindrical tube for a broad range of variation in the enthalpy factor ($0.08 \le \psi_h \le 0.8$).

A diagram of the experimental installation is shown in Fig. 1. We use three plasmatrons (with vortical and magnetic twisting of the arc) – powered by VK-200-6 silicon tubes – to heat the air.

An oscillator with a voltage of 10 kV is used to start the plasmatrons. To prevent rectifier breakdown, at the instant that they were started the plasmatrons were connected to a 200 V dc generator, and the working gas in this case was argon. After the plasmatrons had been started, the power supply was switched to the rectifiers and the argon was replaced by air.

The regulation of the power used to heat the air is achieved by a number of operational plasmatrons, as well as by means of segmented resistance rheostats in an ac circuit. Automatic VAB-20 switches were mounted between the rectifiers and the plasmatrons.

The hot gas leaves the plasmatrons and enters a common water-cooled mixing chamber. As demonstrated by cold-air measurements, the velocity profile at the mixing-chamber outlet was quite uniform. This was achieved with a nozzle exhibiting a convergence ratio of 100:1 and with the plasmatrons positioned in a special way about the mixing chamber to ensure the merging of each of the axes of the twisted jets from the plasmatrons at a single point.

Institute of Thermophysics, Siberian Branch, Academy of Sciences of the USSR, Novosibirsk.
Translated from Inzhenerno-Fizicheskii Zhurnal, Vol. 16, No. 4, pp. 603-609, April, 1969. Original article submitted August 14, 1968.

Subscripts

0 is a scale point for the parameters outside the boundary layer;
t denotes thermal;
w denotes the wall;
φ denotes rotation.

LITERATURE CITED

1. S. S. Kutateladze and A. I. Leont'ev, The Turbulent Boundary Layer of a Compressible Gas [in Russian], Izd. SO AN SSSR, Novosibirsk (1962).
2. A. I. Leont'ev and V. K. Fedorov, Inzh.-Fiz. Zhur., 4, No. 8 (1961).
3. P. N. Romanenko and N. V. Krylova, Inzh.-Fiz. Zhur., 7, No. 4 (1964).
4. S. S. Kutateladze (ed.), Heat and Mass Transfer and Friction in a Turbulent Boundary Layer [in Russian], SO AN SSSR, Novosibirsk (1964).
5. S. S. Kutateladze, A. I. Leont'ev, and A. K. Pimenov, Teplofizika Vysokikh Temperatur, 4, No. 5, 698 (1966).

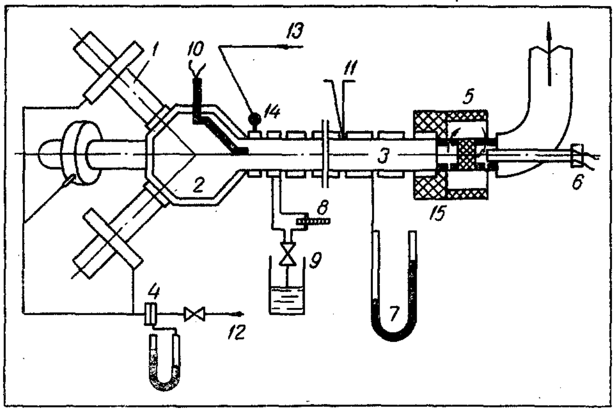

Fig. 1. Diagram of the test installation: 1) plasmatron; 2) mixing chamber; 3) test section; 4) metering disk; 5) mixer; 6 and 10) thermocouples; 7) static-pressure measuring device; 8) device to measure the water temperature at the calorimeter outlet; 9) metering vessel; 11) device to measure wall temperature; 12) air supply; 13) inlet for cooling water; 14) device to measure water temperature at the inlet; 15) thermal insulation.

The test section consisted of a continuous copper tube with an inside diameter of 18.5 mm and a wall thickness of 1.5 mm ($L/D = 51.24$). Copper tubing (5×0.5 in diameter) was wound about certain sections of the tube and fixed with PS-72 solder to form 14 calorimeters of various lengths: (x = 16, 32, 49, 71, 101, 150, 215, 289, 372, 474, 584, 700, 823, 948 mm).

Sleeves were mounted directly at the calorimeter outlet to house the thermometers to measure the water temperature. The calorimeters and the sleeves were insulated with asbestos. The thermometers were graduated for 0.5°C and were calibrated prior to the test. The temperature difference for the water in these experiments was about 30°C for all of the calorimeters. To reduce axial heat leakage, adjacent calorimeter coils were alternately of the inlet and outlet variety.

Chromel–Copel thermocouples 0.1 mm in diameter (to measure wall temperature) were stamped at an angle into the main tube, in the spaces (2-3 mm) between the calorimeters. The static pressure was sampled at these points through orifices 0.5 mm in diameter. These orifices were drilled so as to ensure removal of all burrs from the inside surface of the tube.

The air flow through the test section and the flow rate for the water used to cool the mixing chamber and the plasmatrons were measured by means of the metering disks. The water flow rate was measured through each calorimeter by means of a volume method, the operation being carried out simultaneously for all sections. A constant flow rate was maintained by means of a pressurized tank in which the level was kept constant.

The average temperature for the working air was measured by means of a platinum–platinrhodium thermocouple in a porcelain jacket at the outlet from the test section. We used a porcelain mixer for this purpose, and it simultaneously functioned in the role of a thermal shield for the thermocouple. The enthalpy at the inlet to the test section was calculated from the known air temperature at the outlet and from the total quantity of heat removed from the section. This method had been tested earlier in experiments in which it was possible to measure the air temperature T_{01} at the inlet ($T_{01} \leq 1600$°C) directly by means of a platinum–platinrhodium thermocouple.

The measured and calculated values of T_{01} in these experiments were virtually identical (in certain cases the deviations amounted to 5-7%). This also provided a basis for the assumption that the temperature profile at the inlet to the test section was quite uniform.

To determine the initial energy thickness at the tube inlet (see (5) below) the mixing chamber was calorimetered (the thermometers were graduated for 0.1°C, and the temperature difference for the water was Δt = 3-4°C).

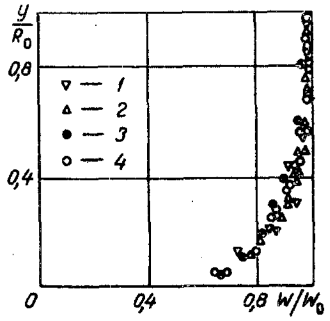

Fig. 2

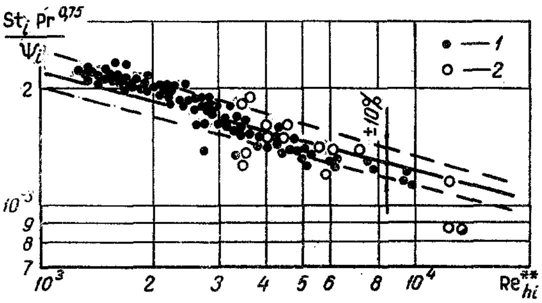

Fig. 3

Fig. 2. Distribution of velocities in the turbulent core at the outlet from the tube, for various instances of nonisothermicity; 1) measurements with a Pitot tube; 2) measurements by means of a tracing method; 3) Nikuradze data, $Re_{d0} = 1.1 \cdot 10^5$ [12]; 1-3) for $\psi_h = 1$; 4) measurements by means of an electron-optical method ($\psi_h = 0.2$).

Fig. 3. The function $St_i Pr^{0.15}/\Psi_i = f(Re^{**}_{hi})$: 1) initial segment; 2) stabilized segment.

Before the main experiments, we determined the heat losses for the test section. Hot water at a temperature of 40°C was fed into the calorimeters for this purpose. These tests showed that the heat losses amount to less than 1%. Prior to each test, we checked the cleanness of the finish on the inside tube surface. Despite some loss of cathode material, the tube surface remained clean.

The tests were carried out in steady regimes, with the voltage at the plasmatron fluctuating no more than ±1%. An M-20 computer was used to reduce the experimental data in the form of the functions

$$\frac{St_i Pr^{0.75}}{\Psi_i} = f(Re^{**}_{hi}), \tag{1}$$

$$St_i = \frac{q_{wi}}{g\rho_0 W_0 \Delta h}, \tag{2}$$

where q_{wi} is the quantity of heat received by each section; Δh is the difference in enthalpy between the tube axis and the wall; ρ_0 and W_0 are, respectively, the density and velocity at the tube axis in the initial segment, and these were found from the measured static pressures P_i by use of the gasdynamic functions

$$\gamma_0 W_0 = \gamma^* W^* q(\lambda_i),$$
$$W^* = \sqrt{\frac{2k}{k+1} gRT_{01}}, \quad \gamma^* = \gamma_{01}\left(\frac{2}{k+1}\right)^{\frac{1}{k-1}}, \quad \lambda_i = f\left(\frac{P_i}{P_{ch}}\right), \tag{3}$$

where P_{ch} is the stagnation pressure in the mixing chamber.

The Reynolds number in (1) is determined from

$$Re^{**}_{hi} = \frac{Re'^{**}_{hi} + Re'^{**}_{h,i+1}}{2},$$

which corresponds to its value at the midpoint of each section. Here Re'^{**}_{hi} and $Re'^{**}_{h,i+1}$ are the values of the numbers corresponding to the initial and final sections of the segment subjected to calorimetry;

$$Re'^{**}_{hi} = \frac{\sum_1^i q_{wi} l_i}{\mu_w \Delta h g} + Re^{**}_{h0}, \tag{4}$$

Re^{**}_{h0} is the initial value for the Reynolds number, defined as

$$Re^{**}_{h0} = \frac{G\Delta t c_p}{\pi D_{ch} \Delta h_{ch} u_w}, \tag{5}$$

where $G\Delta t c_p$ is the quantity of heat removed from the mixing chamber; D_{ch} is the chamber diameter; $\Delta h_{ch} = h_{01} - h_{w\,ch}$; $h_{w\,ch}$ is the enthalpy of the chamber wall; h_{01} is the stagnation enthalpy.

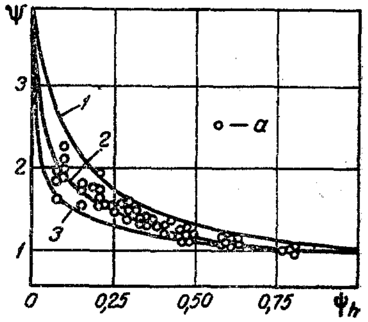

Fig. 4. The function $\Psi = f(\psi_h)$: 1) formula (12); 2) formula (6), $Re_h^{**} = 300$; 3) formula (6), $Re_h^{**} = 10^4$; a) experimental points.

The relative function Ψ_i is found from the equation

$$\psi_h = 1 + \frac{4(1 - \sqrt{\Psi})}{\Psi\left(1 - 8.2\sqrt{cf_0 \Psi \psi_h}\right)}, \tag{6}$$

which was derived in [8]. Here

$$cf_0 = \frac{2}{(2.5 \ln \mathrm{Re}^{**} + 3.8)^2}.$$

The value of Ψ, found from (6), is substituted into (1).

The experimental points in the stabilized segment were processed in the following manner.

The enthalpy difference Δh in (2) for the section x was found from

$$h_{0i} - h_{\mathrm{w}} = \frac{\sum_{1}^{i} q_{\mathrm{w}i} l_i - G_{\mathrm{a}}(h_{01} - h_{\mathrm{w}})}{G_{\mathrm{a}}\left(\frac{1}{\frac{R_0}{2\delta^{**}} - \psi_h \cdot 1.3} - 1\right)}, \tag{7}$$

were h_{0i} is the enthalpy at the tube axis in the stabilized segment.

Equation (7) follows from the energy balance, with consideration of the assumption that $\delta_h^{**} = \delta^{**}$ and

$$\rho_0 W_0 = \frac{\rho_{01} W_{01}}{1 - 2\frac{\delta^*}{R_0}} \approx \mathrm{const}. \tag{8}$$

The integral characteristics of the boundary layer for the main segment were determined from $\omega = \xi^{1/7}$; $\delta^*/\delta^{**} = \psi_h \cdot H_0 = 1.3\,\psi_h$, $\delta = R_0$.

To verify this statement, we measured the velocity profiles at the tube outlet by tracing the flow with minute particles [9-10]. The results show that for Reynolds numbers of Re_h^{**}, which prevail in our experiments, and for the range $1 > \psi_h > 0.1$, the velocity distribution in the turbulent core virtually coincides with the "1/7-th power law" (Fig. 2).

A similar result had been obtained earlier in [7] by means of a pneumometric probe.

The beginning of the main tube segment was found from (7), when

$$\frac{h_{0i} - h_{\mathrm{w}}}{h_{01} - h_{\mathrm{w}}} = 1 \pm 0.01.$$

We can find the values of Re_h^{**} for the main segment by using (8) for this purpose, and also the relationship

$$\delta_h^{**} = \delta_{hH}^{**} \frac{h_{01} - h_{\mathrm{w}}}{h_{0i} - h_{\mathrm{w}}} - \frac{G_{\mathrm{a}}}{\rho_0 W_0 2\pi R_0 g}\left(\frac{h_{01} - h_{\mathrm{w}}}{h_{0i} - h_{\mathrm{w}}} - 1\right) + \frac{2R_0}{(h_{0i} - h_{\mathrm{w}}) g \rho_0 W_0} \int_{\bar{x}_H}^{\bar{x}_i} q_{\mathrm{w}} d\bar{x}, \tag{9}$$

$$\bar{x} = x/2R_0.$$

Equation (9) is derived from the equation of energy for a cylindrical tube:

$$\frac{1}{\gamma_0 W_0 \Delta h R_0} \frac{\partial}{\partial x}\left(R_0 \gamma_0 W_0 \Delta h \delta_h^{**}\right) + \frac{G_{\mathrm{a}}}{\Delta h\, 2\pi R_0 \gamma_0 W_0} \frac{\partial h_0}{\partial x} = \mathrm{St}.$$

Figure 3 shows the experimental data obtained for the initial and stabilized tube segments. Since the values of Re_{hi}^{**} and St_i for the stabilized section in each regime varied only slightly, these data have been plotted in Fig. 3 as the open circles, which represent the average of 3-6 experimental points. Strictly speaking, the proposed method of processing the experimental data for the stabilized segment of the tube is somewhat arbitrary. Nevertheless, the results for the stabilized section in most regimes obey the general quantitative relationship of the curve in Fig. 3, and this is in good agreement with the known relationship

$$\mathrm{St} = \frac{0.0126\,\Psi}{(\mathrm{Re}_h^{**})^{0.25}\,\mathrm{Pr}^{0.75}}. \tag{10}$$

We should point out that a certain indeterminacy in expression (5) may lead to an inaccurate determination of Re_{h0}^{**}, which is noticeable for the values of Re_{hi}^{**} in (4) for the first calorimeters. Nevertheless, this circumstance has virtually no effect on the final result of (10), since the experimental values of St_i are weak functions of the Reynolds $(Re_h^{**})^{0.25}$.

It is demonstrated in [11] that in determining the standard magnitude St_0 on the basis of

$$Re_h^{**} = \frac{W_0 \delta_h^{**} \rho_0}{\mu_w} \tag{11}$$

the experimental points corresponding to the value of the relative Stanton number Ψ for $\psi_h < 1$ group themselves rather tightly about the curve described [1] by the limiting formula

$$\Psi = \left(\frac{2}{\sqrt{\psi_h} + 1}\right)^2, \tag{12}$$

which also follows from (6) as $Re \to \infty$.

Figure 4 shows the experimental data in the coordinates

$$\Psi = f(\psi_h), \quad \Psi = \frac{St_i}{St_0}.$$

The value of St is determined from (2), while that of St_0 is determined from (10) and (11). This curve shows satisfactory agreement with the experiments of other authors whose results are processed in the same way and analyzed in [11], and moreover, it confirms the conclusion drawn in the cited reference as to the possibility of using the limiting formula (12), if St_0 is found with consideration of (11). However, better agreement with the experiment is found in the case of formula (6), when consideration is given to the finiteness of the Reynolds numbers. Calculation on the basis of this formula for $Re_h^{**} = 300$ and 10^4 is shown by curves 2 and 3 in Fig. 4.

NOTATION

$\psi_h = h_w/h_0$	is the enthalpy factor;
$\Psi = St/St_0$	is the relative heat-transfer coefficient;
St_0	is the Stanton number under standard conditions;
q_w	is the heat flow at the wall;
Re_h^{**}	is the Reynolds number, calculated on the basis of the size of the energy loss;
ρ_{01}, W_{01}, ρ_0, and W_0	are, respectively, the density and the velocity at the tube inlet and at the tube axis;
$k = f(T_{01})$	is the adiabatic exponent;
G_a	is the air flow rate;
l_i	is the length of the section;
μ_w	is the coefficient of dynamic viscosity at the temperature of the wall;
$h_{01}-h_w$ and $h_{0i}-h_w$	are, respectively, the enthalpy differences at the axis and at the wall for the initial and main segments;
δ_h^{**} and δ^{**}	are the energy and momentum thicknesses;
R_0	is the tube radius;
$W/W_0 = \omega$	is the dimensionless velocity in the boundary layer;
$Re_{d0} = W_0 2R_0 \rho_{01}/\mu_{01}$	is the Re number on the basis of the inlet parameters;
γ	is the specific weight.

LITERATURE CITED

1. S. S. Kutateladze and A. I. Leont'ev, The Turbulent Boundary Layer of a Compressible Gas [in Russian], Izd. SO AN SSSR, Novosibirsk (1962).
2. V. A. Mukhin, A. S. Sukomel, and V. N. Velichko, Inzh.-Fiz. Zhur., No. 11 (1962).
3. S. C. Sommer, and B. J. Short, J. Appl. Spect., 23, No. 6 (1956).
4. K. Lobb., E. M. Winkler, and J. Persh, J. Appl. Spect., 22, No. 1 (1955).
5. F. K. Hill, J. Aero. Sci., 23, No. 1 (1956).
6. L. V. Kozlov, Izv. Akad. Nauk SSSR, Otd. Tekh. Nauk, No. 2 (1963).
7. N. M. Belyanin, Prikl. Mekhan. Tekh. Fiz., No. 4 (1964).

8. A. I. Leont'ev, B. P. Mironov, and A. V. Fafurin, Prikl. Mekhan. Tekh. Fiz., No. 2 (1969).
9. B. P. Mironov, A. V. Fafurin, and I. L. Kuznetsov, Zhurnal Fizika Goreniya i Vzryva, No. 2 (1967).
10. A. M. Trokhan, I. L. Kuznetsov, G. R. Baranova, and Yu. V. Ignatenko, Zhurnal Goreniya i Vzryva, No. 1 (1966).
11. A. I. Leont'ev and B. P. Mironov, Prikl. Mekhan. Tekh. Fiz., No. 5 (1965).
12. H. Schlichting, Boundary-Layer Theory [Russian translation], IL, Moscow (1956).